

## 9– NMR Interactions: Quadrupolar Coupling

### 9.1 Hamiltonian

The quadrupolar interaction is an interaction between the nuclear spin  $I \geq 1$  and the electric field surrounding it, created by the charges around the nucleus in question. The quadrupolar interaction is a tensor quantity which depends on the electric field gradient (EFG)  $\mathbf{V}$ :

$$\mathbf{Q} = \frac{eQ\mathbf{V}}{2I(2I - 1)\hbar} \quad (9.1)$$

where  $Q$  is the electric quadrupolar moment,  $I$  is the spin quantum number,  $e$  is the charge of the electron and finally the EFG  $\mathbf{V}$  is given by

$$\mathbf{V} = \begin{pmatrix} V_{xx} & 0 & 0 \\ 0 & V_{yy} & 0 \\ 0 & 0 & V_{zz} \end{pmatrix} \quad (9.2)$$

in the principal axis system (PAS) of the EFG. As with the CSA, there are a number of definitions associated with the EFG, such as

$$V_{xx} + V_{yy} + V_{zz} = 0 \quad (9.3)$$

which is analogous to the equation of the CSA tensor parameters.

Also,

$$|V_{zz}| \geq |V_{xx}| \geq |V_{yy}| \quad (9.4)$$

and one can define an asymmetry parameter  $\eta$

$$\eta = \frac{V_{yy} - V_{xx}}{V_{zz}}. \quad (9.5)$$

The quadrupolar coupling constant is given by

$$\chi = \frac{e^2 Q q_{zz}}{h} \quad (9.6)$$

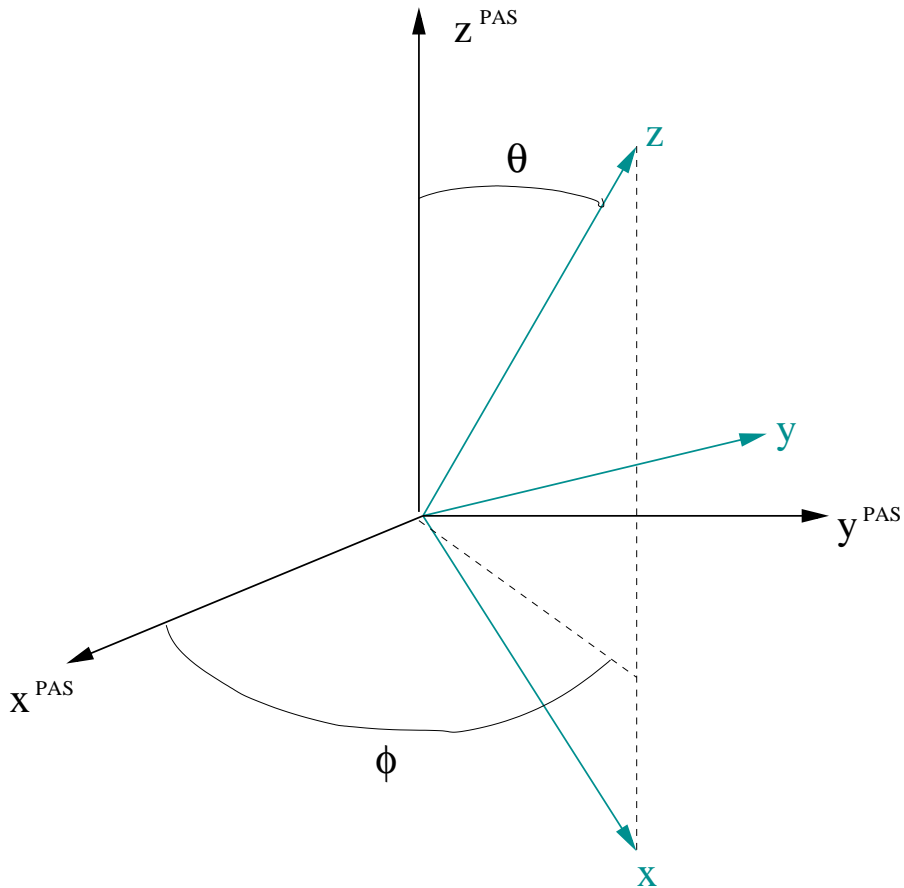
where  $eq_{zz}$  corresponds to the largest principal component of the EFG, i.e.  $V_{zz}$ . As a result of the quadrupolar interaction, the lines observed in spectra of quadrupolar nuclei are split by  $\Delta\nu_Q$

$$\Delta\nu_Q(\theta, \phi) = \frac{1}{2}\nu_Q[3\cos^2\theta - 1 - \eta\sin^2\theta\cos 2\phi] \quad (9.7)$$

where

$$\nu_Q = \frac{3\chi}{2I(2I - 1)}. \quad (9.8)$$

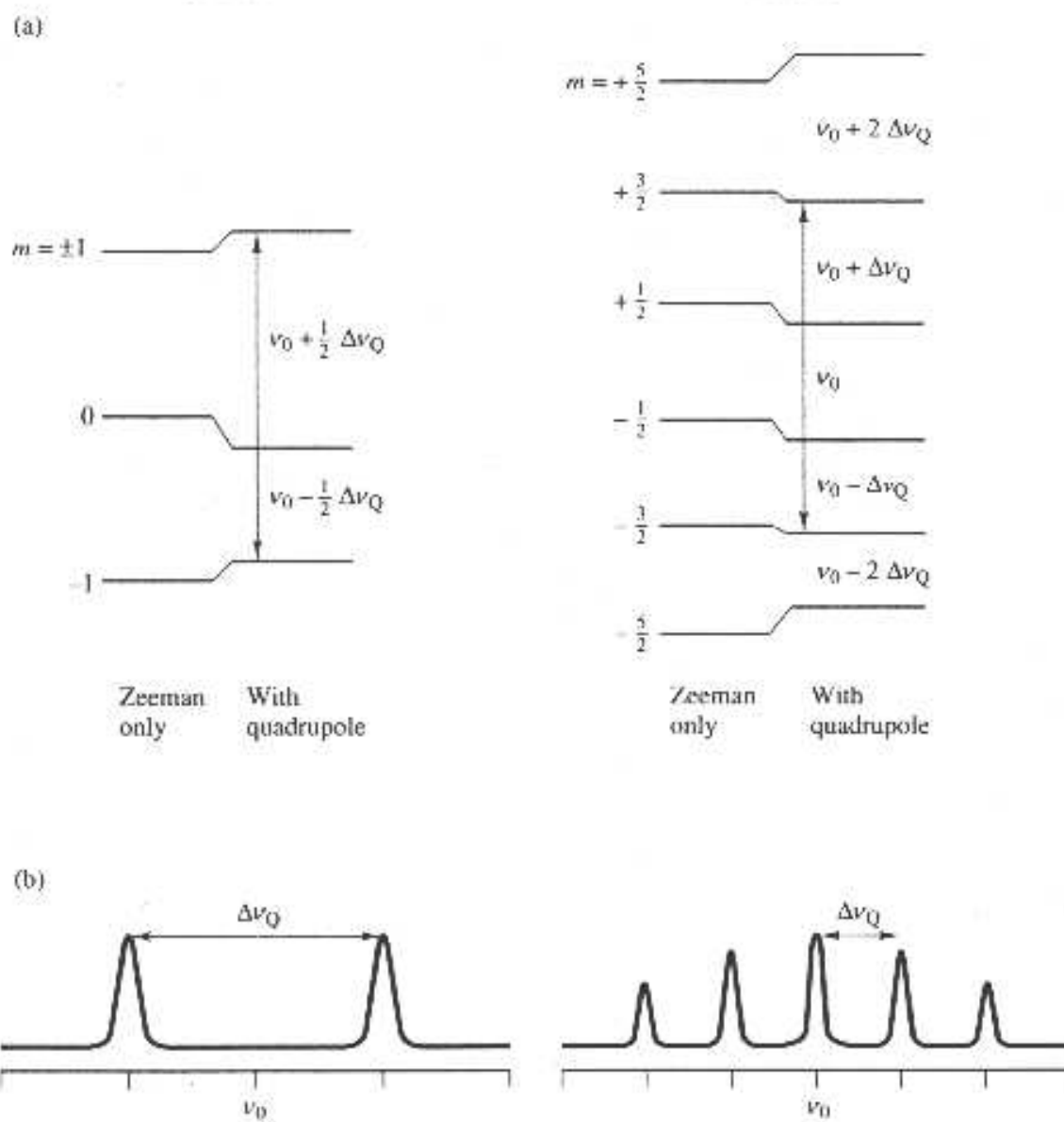
and  $\theta$  and  $\phi$  are defined as



The energy levels are given by

$$\Delta E_m = \frac{1}{4\pi} \Delta\nu_Q(\theta, \phi) \left[ m^2 - \frac{1}{3} I(I+1) \right], \quad (9.9)$$

i.e. for  $I = 1$  and  $I = 5/2$



(ref.: A.J. Vega, Encyclopedia of NMR, Grant and Harris (eds.))

with  $m$  as defined in lecture 1.

Since the quadrupolar coupling is often on the order of hundreds of kHz to several MHz, this represents a significant change in the energy levels.

The full quadrupolar Hamiltonian is given by

$$\begin{aligned}
 \hat{\mathcal{H}}_Q &= \frac{3eQ}{4I(2I-1)\hbar} [V_{zz}(3\hat{I}_z^2 - \vec{\hat{I}} \cdot \vec{\hat{I}}) \\
 &+ (V_{xx} - V_{yy})(\hat{I}_x^2 - \hat{I}_y^2) \\
 &+ 2V_{xy}(\hat{I}_x\hat{I}_y + \hat{I}_y\hat{I}_x) \\
 &+ 2V_{xz}(\hat{I}_x\hat{I}_z + \hat{I}_z\hat{I}_x) \\
 &+ 2V_{yz}(\hat{I}_y\hat{I}_z + \hat{I}_z\hat{I}_y)]. \quad (9.10)
 \end{aligned}$$

As with the quadrupolar interaction, we can make a secular approximation, i.e. at high fields:

$$\hat{\mathcal{H}}_Q = \frac{3eQ}{4I(2I-1)\hbar} [V_{zz}(3\hat{I}_z^2 - \vec{\hat{I}} \cdot \vec{\hat{I}})] \quad (9.11)$$

i.e. only the first is preserved.

## 9.2 Averaging the Quadrupolar Interaction

In past chapters, we have mentioned that in solution, anisotropic parameters are averaged by isotropic

tumbling. This also holds for the quadrupolar interaction. For solids, however, we saw that we need to use magic angle sample spinning to remove anisotropic interactions such as the CSA and the dipolar interaction, which both have a  $3\cos^2\theta - 1$  dependence. For the quadrupolar interaction, we have a dependence on zero, second- and fourth-order Legendre Polynomials  $P_n(\cos\theta)$ , where  $n = 0, 2$  and  $4$ , i.e.

$$\begin{aligned}
 P_2(\cos\theta) &= (3\cos^2\theta - 1) \\
 P_4(\cos\theta) &= (35\cos^4\theta - 30\cos^2\theta + 3)
 \end{aligned}
 \tag{9.12}$$

The averaged value for  $\nu_Q$  under sample rotation,  $\langle \nu_Q \rangle_{rot}$  is given by

$$\langle \nu_Q \rangle_{rot} = A_0 + A_2 P_2(\cos\beta) + A_4 P_4(\cos\beta) \tag{9.13}$$

where  $A_0$  is the isotropic shift, and  $A_2$  and  $A_4$  are functions of  $\omega_Q$ ,  $\omega_0$ ,  $\eta$  and the relative orientation of the quadrupolar tensor and rotor axis.  $\beta$  is the angle between the rotor axis and the static magnetic field  $\vec{B}_0$ .  $P_2(\cos\beta)$  and  $P_4(\cos\beta)$  are averaged to zero and

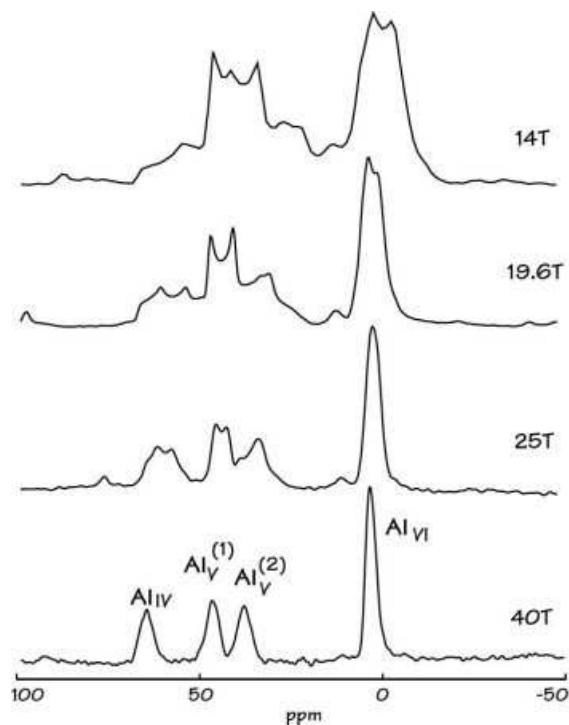
$-7/18$ , respectively, for sample rotation at the magic angle. Hence MAS only reduces the linewidths of the resonances obtained from powdered samples by approximately  $1/3$ , and for large  $\chi$  significant second-order quadrupolar line broadening remains.

So in order to remove the quadrupolar interaction, we must do more than just use MAS.

There are three major ways to reduce or remove the quadrupolar interaction.

## 1- High Fields

The most straightforward approach is to work at as high fields as possible, since the broadening is inversely proportional to  $\omega_0$ .



## 2-Mechanical Averaging

Two techniques are possible: dynamic angle spinning (DAS) or double rotation (DOR).

In DOR, averaging of the second-order quadrupolar broadening can be achieved by simultaneously spinning at two angles. These angles,  $\beta_1$  and  $\beta_2$ , are chosen such that both the second- and fourth-order Legendre polynomials are reduced to zero, i.e.

$$\begin{aligned}\beta_1 &= \arccos(1/\sqrt{3}) \\ \beta_2 &= 30.55^\circ \\ \text{or } \beta_2 &= 70.12^\circ.\end{aligned}\tag{9.14}$$

In practice this is achieved with a small rotor containing the sample (the inner rotor) which spins inside another rotor (the outer rotor). The axis of rotation of the inner rotor is inclined at an angle of 30.55 degrees to the axis of rotation of the outer rotor. The outer rotor is then spun at the magic angle. A major limitation to the technique remains the spinning speed of the outer rotor: speeds of not more than 1.2 kHz are typically achieved, and the

spectra often contain many overlapping resonances. The DAS experiment works by spinning separately about two DAS complementary angles such that the second-order quadrupolar broadening is of equal magnitude for the two angles, but opposite in sign. A 2-dimensional experiment is performed, where the spins are returned to the z-direction to preserve the magnetization while the flip between the two angles is implemented (mechanically flip the rotor to different angles). The evolution due to  $\nu_Q$  is refocused when  $t_1 = t_2$ , and an echo forms. Data acquisition is started at the echo maximum at  $t_2$ . A Fourier transform along  $t_1$  yields the isotropic resonance, and quadrupolar second-order lineshapes are obtained after a Fourier transform along  $t_2$ . The DAS complementary angles can be found by finding solutions to the two simultaneous equations:

$$\begin{aligned}
 P_2(\cos\beta_1) + kP_2(\cos\beta_2) &= 0 \\
 P_4(\cos\beta_1) + kP_4(\cos\beta_2) &= 0
 \end{aligned}
 \tag{9.15}$$

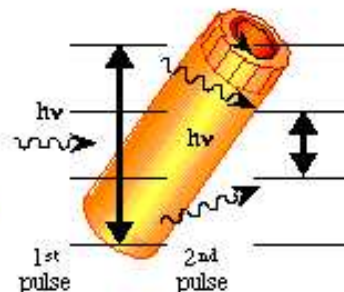
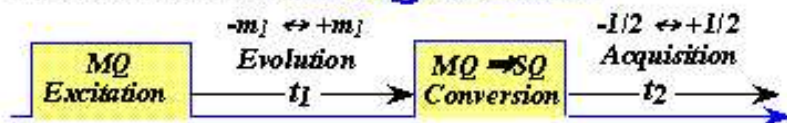
For example, when  $k = 5$ ,  $\beta_1 = 0^\circ$ , and  $\beta_2 = 63.32^\circ$  and an echo will be produced at  $5t_1 = t_2$ .

DAS is only effective for nuclei with sufficiently long spin-lattice relaxation times, so that significant magnetization is not lost during the time used to flip the rotor. In addition, DAS will not remove the homonuclear dipolar couplings (why not?). Since this is a 2D experiment, experiment times are typically longer than for DOR.

## Multiple Quantum MAS NMR

In addition to the central transition, all odd-order multiple quantum (MQ) transitions of quadrupolar nuclei (i.e. 3Q, 5Q etc.) are unaffected by the first-order quadrupolar interaction. These MQ transitions are not directly observable, but can be observed indirectly if the MQ coherence is transferred back to the observable single (1Q) coherence, using the following pulse sequence:

The resulting experiment : **2D MQMAS NMR**



The MQ transitions are affected to second-order by the quadrupolar interaction,  $\nu_Q(2)$ , by an amount that depends on the order of coherence. Both the  $A_2$  and  $A_4$  terms defined above depend on the order of coherence. For example  $A_4(1)/A_4(3) = -54/42$  for  $I = 3/2$ , where  $A_4(1)$  and  $A_4(3)$  are the  $A_4$  terms for the 1Q and 3Q coherences, respectively. Frydman et al. demonstrated that the dependence of  $\nu_Q(2)$  on coherence order could be exploited to average the second-order interaction and thus developed the MQMAS experiment.

The experiment is performed under conditions of MAS, so that the  $A_2P_2(\cos\beta)$  terms are averaged to zero. Averaging of the  $A_4P_4(\cos\beta)$  terms is then achieved by allowing the spins to evolve for different time periods in the single and multiple quantum time dimensions,  $t_{1Q}$  and  $t_{MQ}$ , respectively, such that the  $A_4$  terms average to zero, i.e., for  $I=3/2$ ,  $t_{1Q}/t_{3Q} = 42/54$ . The experiment can be considered analogous to DAS, except that now the averaging is achieved by allowing the spins to evolve in two different MQ coherences; the experiment is

also performed in a similar fashion. A single pulse is used to excite the 3Q (or MQ) transition, in the simplest form of this experiment. Appropriate phase cycling is used to select the order of MQ coherence (e.g., 3, or 5). The spins are allowed to evolve for  $t_1$ , whereupon the 3Q coherence is then converted to a 1Q coherence (i.e., observable magnetization). Echo formation occurs in the  $t_2$  dimension, when the  $A_4$  terms cancel. Performing the Fourier transform along the echo maximum, as a function of  $t_1$ , provides a spectrum free from second-order quadrupolar broadening. A Fourier transform performed in a direction perpendicular to the echo, provides the second-order lineshape. A shearing transformation can be applied to the data,  $S(t_1, t_2)$ , that rotates the 2D FID, so that the isotropic and anisotropic spectra are observed in  $\omega_1$  and  $\omega_2$ , respectively, after the Fourier transform. The method is relatively straightforward to implement on a conventional MAS probe, and does not require any additional hardware, thus, there have already been a considerable number of applications of this experiment to quadrupolar systems.

### 9.3 Effect of Quadrupolar I on I=1/2

If a spin  $I_1 = 1/2$  is directly bonded to a spin  $I_2 \geq 1$ , then the dipolar interaction between these two spins may acquire an orientational dependence which cannot be averaged out by MAS (cf. Dipolar interaction section). This effect can be observed for spins  $I_2$  with large quadrupolar coupling constants  $\chi$ , since in this case the magnitude of the quadrupolar coupling constant ( $\chi = 1 - 10\text{MHz}$ ) is not significantly different from the static magnetic field ( $B_0 = 100\text{sofMHz}$ ).

Recall from the first lecture that NMR experiments are usually run with the assumption that the high temperature approximation is valid, i.e. that the thermal energy of the system is greater than the magnetic energy

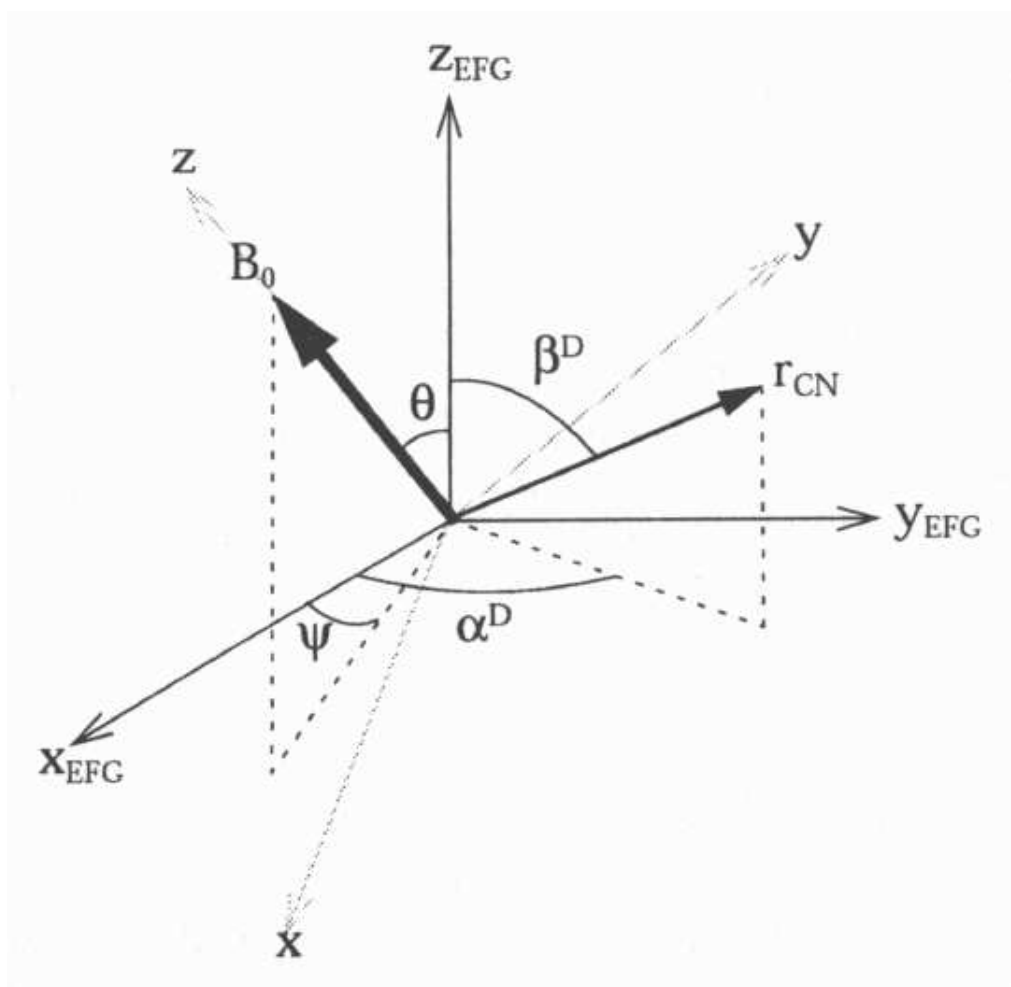
$$\gamma h J B_0 \ll 2\pi kT. \quad (9.16)$$

In the case where  $\chi \approx B_0$ , this relation is no longer valid since the energy levels are no longer quantized along the external field  $B_0$ , but rather along a different field which encompasses both  $B_0$  and  $\chi$ .

As a result of this effect, the line for the spin  $I_1 = 1/2$  is split by

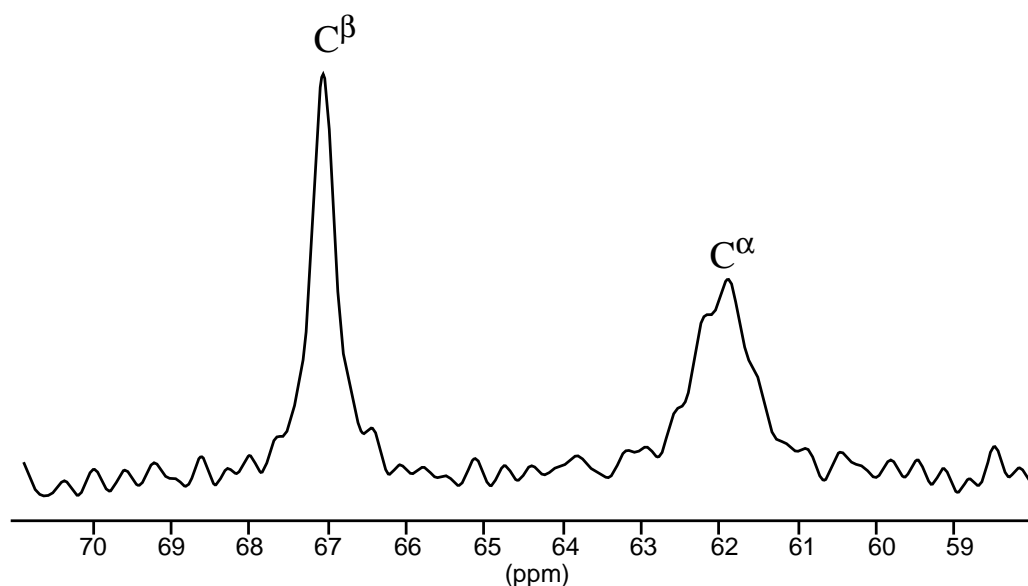
$$S = \frac{9}{20} \frac{d_{I_1 I_2} \chi}{2\pi |\omega_{0, I_2}|} [(3 \cos^2 \beta^D - 1) + \eta \sin^2 \beta^D \cos 2\alpha^D], \quad (9.17)$$

with the angles defined as



For a  $^{13}\text{C} - ^{14}\text{N}$  pair, separated by a distance of  $r_{CN} = 1.46$  angstroms and  $|\chi| = 3.0\text{MHz}$ , the

splitting  $S$  is 39 Hz at 9.4T and around 50 Hz at 7.0T. The spectrum below shows an experimental  $^{13}\text{C}$  spectrum for unlabelled threonine. Though both  $\text{C}^\beta$  and  $\text{C}^\alpha$  are CH groups in this amino acid, the intensity of the lines are markedly different and the  $\text{C}^\alpha$  line is split by approx. 50 Hz.



In order to eliminate this splitting, decoupling methods specially designed for quadrupolar nuclei would need to be used. Examples include overtone decoupling and dynamic angle spinning (DAS). See A.J. Vega, Encyclopedia of NMR, Grant and Harris (eds.) for more details.

Note that since the splitting  $S$  is inversely proportional to the static magnetic field strength  $B_0$ ,

this effect becomes smaller at larger magnetic fields.

## 9.4 Importance of the Quad. Interaction

1. Most nuclei are quadrupolar!!!

*Most abundant isotopes in the periodic table*

H																	He		
Li	Be	<b>SPIN-1/2</b>												B	C	N	O	F	Ne
Na	Mg	<b>HALF-INTEGER QUADRUPOLAR SPINS</b>												Al	Si	P	S	Cl	Ar
K	Ca	Sc	Ti	V	Cr	Mn	Fe	Co	Ni	Cu	Zn	Ga	Ge	As	Se	Br	Kr		
Rb	Sr	Y	Zr	Nb	Mo	Tc	Ru	Rh	Pd	Ag	Cd	In	Sn	Sb	Te	I	Xe		
Cs	Ba	La	Hf	Ta	W	Re	Os	Ir	Pt	Au	Hg	Tl	Pb	Bi	Po	At	Rn		
Fr	Ra	Ac																	
			Ce	Pr	Nd	Pm	Sm	Eu	Gd	Tb	Dy	Ho	Er	Tm	Yb	Lu			
			Th	Pa	U	Np	Pu	Am	Cm	Bk	Cf	Es	Fm	Md	No	Lr			

- In solution, though the quadrupolar interaction is averaged (because all  $\theta$ 's and  $\phi$ 's are sampled), it can still play a role in relaxation.
- In solids, the quadrupolar interaction is used to

get dynamic and orientational information:

e.g. Dynamics

Since quadrupolar nuclei have very broad lineshapes, they serve as good probes for studying the dynamics of different moieties. The lineshape is very sensitive to changes in the motion within the molecule as illustrated in the two examples below:

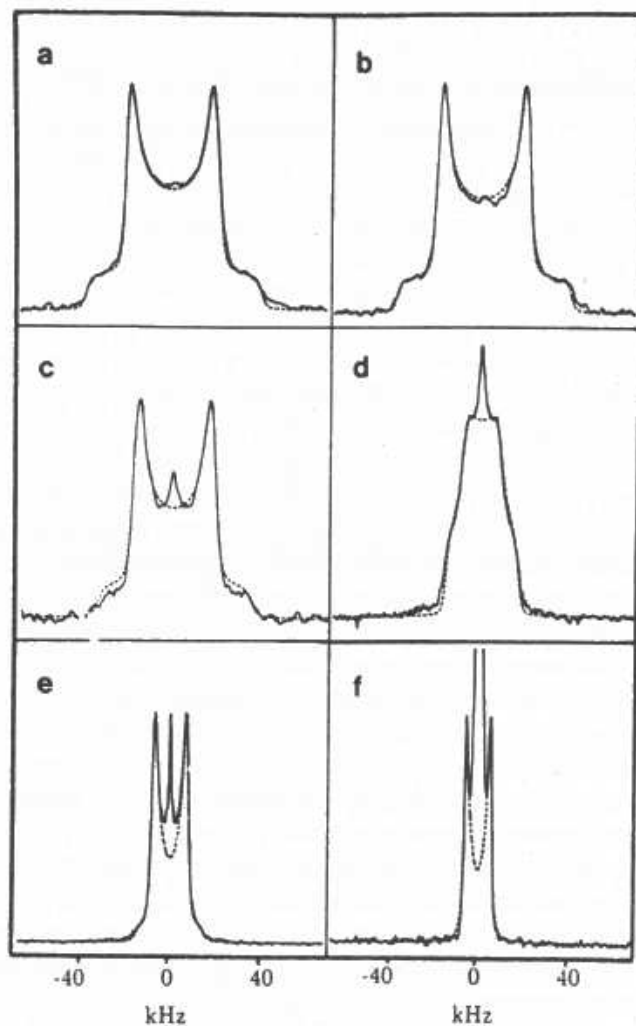


**Figure 24.** Experimental (—) and simulated (---) 76.75-MHz deuterium quadrupole echo spectra of [methyl- $^2\text{H}$ ]-2'-deoxythymidine-labeled  $[\text{d}(\text{CGCGAAT}^*\text{T}^*\text{CGCG})_2]$  at various hydration levels  $W$  (mol of  $\text{H}_2\text{O}$ /mol of nucleotide). The simulated spectra were calculated as described in text, ignoring the central isotropic component. Spectra for pulse delay of  $50 \mu\text{s}$  at (A) dry lyophilized powder,  $W \approx 0$ , 12 000 scans; (B) 75% RH,  $W = 10.4$ , 24 000 scans; (C) 88% RH,  $W = 16.3$ , 32 000 scans; (D) 90% RH,  $W = 21.2$ , 28 500 scans; (E) 92% RH,  $W = 26.6$ , 32 000 scans; (F) 95% RH,  $W = 39.8$ , 8000 scans.

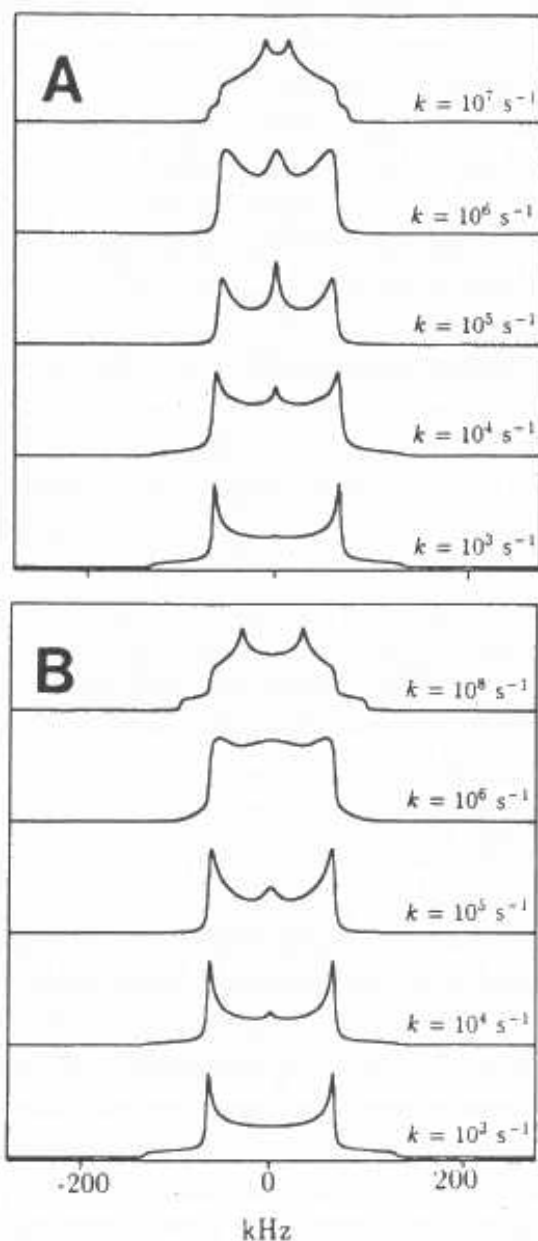


**Figure 30.** Simulations of backbone conformational conversions for a pulse delay of  $50 \mu\text{s}$  as a function of jump rate  $k_{ij}$ . (A) Interconversion between gauche-gauche (+sc), gauche-trans (ap), and trans-gauche (-sc) with populations of 0.85 (site 1), 0.05 (site 2), and 0.10 (site 3), respectively. The site to site jump rates  $k_{12}$ ,  $k_{13}$ , and  $k_{2,3}$  were assumed to be equal. (B) Two-site diamond lattice jump with site population of 0.8 and 0.2 for differing jump rates  $k_{12}$ .

ref: T.M. Alam and G.P. Drobny, *Chemical Reviews*, **91**, 1545-1590 (1991).